

Observational bounds on a possible electron-to-proton mass ratio variation and constraints in the lepton-specific 2HDM

R. G. Albuquerque^{1,*}, R. F. L. Holanda^{2,3,4,†}, I. E. T. R. Mendonça^{2,5,‡} and P. S. Rodrigues da Silva^{1,§}

¹*Departamento de Física, Universidade Federal da Paraíba,
Caixa Postal 5008, 58051-970, João Pessoa, PB, Brasil*

²*Departamento de Física, Universidade Federal do Rio Grande do Norte,
Natal - Rio Grande do Norte, 59072-970, Brasil*

³*Departamento de Física, Universidade Federal de Campina Grande, 58429-900, Campina Grande - PB, Brasil*

⁴*Departamento de Física, Universidade Federal de Sergipe, 49100-000, Aracaju - SE, Brazil and*

⁵*Biofy.tech IA Department, 38407-180, Uberlândia-MG Brazil*

In this work, we test a possible redshift variation of the electron-to-proton mass ratio, $\mu = m_e/m_p$, directly from galaxy cluster gas mass fraction measurements and type Ia Supernovae observations. Our analysis is completely independent of any cosmological model. Our result reveals no variation of μ within 1σ confidence level. From the point of view of Particle Physics, we can use the precision on these results to constrain the parameter space of models beyond the Standard Model of electroweak interactions. We exemplify this by focusing in a specific Two Higgs Doublet model (2HDM), where the second scalar doublet couples exclusively to leptons. An important parameter in the model concerns the ratio between its vacuum expectation values, defined by $\tan\beta$. In our approach we can constrain the inverse parameter ($\cot\beta$) to an optimal value, $(\tan\beta)^{-1} = 0.02127 \pm 0.0029$, with the largest vacuum expectation value for 2HDM, v_2 , estimated at around 240.033 ± 0.21 GeV. Also, by taking into account the $(g-2)_\mu$ discrepancy found between theory and experiment, we can reduce the validity region for this model and establish bounds on the scalar masses, in the light of our findings from galaxy clusters data for μ . This study contributes valuable insights to the understanding of Particle Physics and Astrophysics interface, establishing a new interplay between data from large scale structure of the Universe and subatomic Physics.

PACS numbers: 98.62.Ra, 98.65.-r, 98.80.-k, 12.60.Fr, 14.80.Ec

I. INTRODUCTION

Fundamental physical theories rely on certain parameters known as fundamental constants, for instance the fine structure constant, gauge and Yukawa couplings, and so on. Their values cannot be predicted from existing knowledge and must be determined through experimentation. We assume these constants are mathematical constructs and to be unchanging across both time and space, according to the simpler successful physical theories. Dirac [1] was among the first to question whether these constants are merely mathematical constructs or if they hold deeper significance within a broader cosmological framework. Current laboratory experiments have ruled out significant variations in these constants over laboratory [2], geological [3, 4], and solar system time scales [5]. Astrophysical methods, specifically, the spectroscopy of quasar absorption lines which involve measuring transition wavelengths at high redshifts over vast time intervals, probe a much wider span of time [6–9].

In recent years, observational tests seeking possible variations in fundamental constants have grown in the literature (see [10–13] for a review). In this scenario, two dimensionless constants, the fine structure constant, ($\alpha \equiv e^2/4\pi\epsilon_0\hbar c$), and the electron-to-proton mass ratio, ($\mu \equiv m_e/m_p$), hold particular importance as these constants are not only related to each other, but their possible variation is also linked to new physics such as: models of extended gravity[14–16], string theory [17, 18], and more recently, dark matter models [19, 20]. Therefore, constraining the temporal and spatial change of these parameters could profoundly impact both cosmology and fundamental physics. The use of physics of large scale structure of the universe, i.e., the physics of galaxy clusters, to constrain variations on α is not new [21], nevertheless, it has been a field of intense investigation recently [22–27]. On the other hand, as far as we are aware, there have been no report on the issue of μ variation using galaxy clusters until now, a path we are going to follow in this work.

*Electronic address: rennangomes@outlook.com

†Electronic address: holandarfl@fisica.ufrn.br

‡Electronic address: isaacmendonca@biofy.tech

§Electronic address: psilva@fisica.ufpb.br

Concerning the physics of small scale, the Standard Model of Strong and Electroweak interactions (SM) has been thoroughly confirmed along the past decades by several collider data measurements, culminating with the last important ingredient predicted by the model and discovered at the large Hadron Collider (LHC), namely, the Higgs boson [28–30]. It was an important step to definitely establish the SM as a fiducial paradigm for describing the visible matter content in the Universe and its interactions in a detailed and precise way. However, it is not the most complete theory we can envisage. That is because we know there are several issues, like the evidence for Cold Dark Matter [31], neutrino’s mass and oscillation [32, 33], the experimental deviation from the theoretical prediction of the muon anomalous magnetic moment [34, 35], etc, that cannot be addressed by the model without extending its matter or interaction content (gauge group). In this sense, several models have been proposed in literature to go beyond SM, but a class of such models is being particularly of interest for phenomenologists as the scalar sector of the SM is being scrutinized, the so called Two Higgs Doublet Models (2HDM) [36, 37]. An extra doublet scalar is the simplest part of supersymmetric theories¹ content that can be theoretically studied without, necessarily, addressing specific details of the intricate spectrum of such theories. Besides, 2HDM can add sources of CP violation in the scalar sector [41], allowing for Baryogenesis in this class of models [42, 43], and the extra neutral scalar can offer a richer vacuum structure that could lead to a first order phase transition [44–47], also required for Baryogenesis. Finally, it is well known that additional scalar doublets do not alter the SM prediction for the observable ρ -parameter².

Our main goal in this work is to impose constraints on a possible redshift variation of electron to proton mass ratio, μ , by using observational data, more precisely, galaxy cluster gas mass fraction data and SNe Ia luminosity distance measurements, and put constraints on particle physics models beyond the SM. We do that for a specific version of 2HDM, where leptons and quarks interact with different scalar doublets. Since the constraint on μ from galaxy clusters is directly related to the ratio between the vacuum expectation values (vev) of the model³, we can use the constraint on μ , to get bounds on the parameters of the 2HDM. In order to impose tighter limits in the parameter space, including the scalar masses of the model, we also perform the computation of the muon anomalous magnetic moment, restricting to the region of parameters that can solve the 4.2σ discrepancy between experiment and theory that presently seems a promising indication for physics beyond the SM [48].

The manuscript is organized as follows: we first present the methodology by which we derive the relation between the electron-to-proton mass ratio and the galaxy cluster gas mass fraction in Section II. Then, in Section III, we briefly explain the cosmological data sample used in our analysis. We describe, in Section IV, the theoretical structure of the 2HDM that we base our investigation on. In Section V we describe the details of our analysis and the results we get for the μ variation. After that, in Section VI, we present constraints on $\tan\beta$, as well as the masses of the heavier Higgs in the 2HDM, including the computation of the muon anomalous magnetic moment contribution to solve the theoretical-experimental discrepancy. Finally we draw our conclusions and share some perspectives in Section VII.

II. ELECTRON-TO-PROTON MASS RATIO AND GALAXY CLUSTER GAS MASS FRACTION

Galaxy clusters represent the largest virialized structures in the universe [49]. Predominantly composed of dark matter and intergalactic gas in a plasma state known as the Intra-Cluster Medium (ICM), which emits a continuous X-ray spectrum. The spectrum is dominated by thermal bremsstrahlung for temperatures from 2 – 10 keV[50]. The ratio of ICM mass to the total cluster mass, i.e., the gas mass fraction f_{gas} , holds particular significance in cosmology, since it allows to constrain cosmological parameters [51–53]. Moreover, it enables various tests on the fundamental physics, including, for instance, the exploration of fundamental constant variations [24, 54] and violations of Einstein’s equivalence principle [55–57]. Consider the gas mass, M_{gas} , within a radius R , obtained through X-ray spectrum measurements [50, 58]:

$$M_{gas}(< R) = \left(\frac{3\pi\hbar m_e c^2}{2(1+X)e^6} \right)^{1/2} \left(\frac{3m_e c^2}{2\pi k_B T_e} \right)^{1/4} m_H \times \frac{1}{[\bar{g}_B(T_e)]^{1/2}} r_c^{3/2} \left[\frac{I_M(R/r_c, \beta)}{I_L^{1/2}(R/r_c, \beta)} \right] [L_X(< R)]^{1/2}. \quad (1)$$

Here, X is the fraction of Hydrogen mass in the gas, m_e and m_H are the masses of the electron and Hydrogen, respectively. T_e is the gas temperature, \bar{g}_B is the Gaunt factor, multiplicative correction to take quantum effects in

¹ Supersymmetric theories (for a review, see Ref. [38–40] and references therein) are thoroughly investigated for decades since it is a fundamental piece for the mathematical consistency of string theory, although no sign of it has shown up in accelerators till now.

² The ρ -parameter is defined (at tree level) as $\rho_{tree} = \frac{M_W^2}{M_Z^2 \cos^2 \theta_W}$, where M_W and M_Z are the W and Z weak gauge bosons’ masses, respectively, and θ_W is the weak mixing angle. Its theoretical value in the SM is $\rho_{tree} = 1$.

³ As we will see, in our approach we restrict to the variation of electron mass only in the electron-to-proton mass ratio, and that alone allows us to infer that the ratio of vevs of 2HDM, namely, $\tan\beta$ is the parameter to be constrained by the μ variation.

consideration for the calculations of absorption or emission of radiation [59], and r_c is the core radius. I_M and I_L are defined as:

$$I_M(y, \beta) \equiv \int_0^y (1+x^2)^{-3\beta/2} x^2 dx,$$

$$I_L(y, \beta) \equiv \int_0^y (1+x^2)^{-3\beta} x^2 dx,$$

obtained using a spherical β model, and the bolometric luminosity $L_X(< R)$ is given by:

$$L_X(< R) = 4\pi[D_L(z, \Omega_0, H_0)]^2 f_X(< \theta) ,$$

where $f_X(< \theta)$ is the total bolometric flux within the outer angular radius θ [60]. D_L is the luminosity distance, which depends on redshift, z , and cosmological densities parameters, Ω 's, and the Hubble parameter, H_0 . The total cluster's mass M_{tot} , obtained by using the Euler equation for a fluid in hydrostatic equilibrium, with the additional assumption of isothermality [61], is given by:

$$M_{tot}(< R) = - \left. \frac{k_B T_e R}{G x_H m_H} \frac{d \ln n_e(r)}{d \ln r} \right|_{r=R} . \quad (2)$$

Here, x_H is the molar fraction of hydrogen in the gas, G is Newton's gravitational constant and n_e is the electron gas density. Thus, from Eq.(1), we observe that $M_{gas} \propto m_H$, and from Eq.(2), $M_{tot} \propto 1/m_H$. Consequently, we can conclude that the gas mass fraction, f_{gas} within the intra-cluster medium which is the ratio between Eq.(1) and Eq.(2),

$$f_{gas} \propto m_H^2, \quad (3)$$

and since $m_H = m_e + m_p$, then

$$f_{gas} \propto (1 + \mu)^2 m_p^2, \quad (4)$$

Which as we can see, explicitly depends on μ , the ratio of electron to proton masses.

On the other hand, the expected constancy of the f_{gas} within massive, hot and relaxed galaxy clusters with redshifts in the interval of interest has been used to constrain cosmological parameters via the following equation [51–53]:

$$f_{gas}^{th}(z) = \gamma(z) K(z) A(z) \frac{\Omega_b}{\Omega_m} \left[\frac{D_L^*}{D_L} \right]^{3/2} . \quad (5)$$

In the previous Eq.(5), D_L^* indicates the luminosity distance calculated using a fiducial concordance model, D_L is the distance of interest, and $\gamma(z)$ is the baryon depletion factor, which for our purposes and conservatively, can be taken as the best value $\gamma_0 = 0.799 \pm 0.11$ independent of z [62, 63]. Ω_b and Ω_m are the baryonic and matter abundances density parameters, respectively, $K(z)$ is the mean ratio of lensing to X-ray mass, which too, can be taken at best value: $K_0 = 0.96 \pm 0.12$ independent of z [53] and $A(z)$ represents the angular correction factor, which is close to unity for all cosmologies and redshifts of interest, and it can be neglected without significant loss of accuracy [64]. Thus, considering a possible variation of μ with redshift, we modify Eq.(5) accordingly, arriving at the expression:

$$f_{gas}^{obs} = (1 + \mu(z))^2 \gamma K A \frac{\Omega_b}{\Omega_m} \left[\frac{D_L^*}{D_L} \right]^{3/2} . \quad (6)$$

Finally, if the luminosity distance is known for each galaxy cluster, $\mu(z)$ can be inferred through the deviation from zero of $(1 + \mu)^2$ with respect to the ratio $\frac{f_{gas}^{obs}}{f_{gas}^{th}}$,

$$(1 + \mu)^2 - \frac{f_{gas}^{obs}}{f_{gas}^{th}} = 0 , \quad (7)$$

where f_{gas}^{obs} is the gas mass fraction dataset⁴ presented in Section III and f_{gas}^{th} comes from Eq (5). This will provide 44 values of μ , which will be used to reconstruct the function $\mu(z)$ via Gaussian process regression, as we describe next.

⁴ Which would be equivalent to the modified equation for f_{gas} .

III. COSMOLOGICAL DATA

A. Gas Mass Fraction

We utilize the most new sample of f_{gas} measurements spanning the redshift range $0.018 \leq z \leq 1.160$, compiled in Ref. [65]. This dataset comprises 44 massive, hot, and morphologically relaxed galaxy clusters observed by the Chandra telescope (see Fig.1). The selection of relaxed systems aims to minimize systematic biases in the hydrostatic masses. The gas mass fraction is computed within the spherical shell defined by $0.25 \leq r/r_{2500} \leq 0.8$ rather than integrated at all radii. Further details about the data can be found in Ref. [53, 65]. In order to perform a cosmological model independent analysis, the Ω_b/Ω_m ratio utilized is from galaxy clustering observations as given by [66], such as: $\Omega_b/\Omega_m = 0.173 \pm 0.027$. Conversely, the majority of cosmological constraints derived from observations of gas mass fraction in X-ray emitting sources are dependent on hydrodynamic simulations [67, 68].

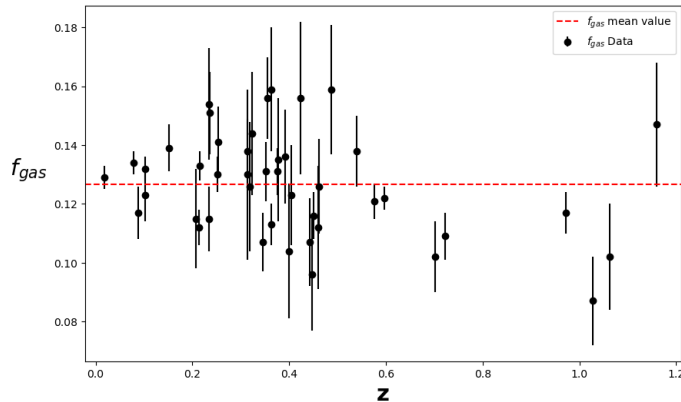


FIG. 1: The 44 Chandra X-ray gas mass fraction as a function of redshift compiled by Mantz et al. [65].

B. SNe Ia sample

As formerly discussed, in order to perform our test, we need the luminosity distance for each galaxy cluster. Then, we consider the PANTHEON dataset of Type Ia supernovae, compiled in 2018 by Scolnic et al. [69], which is a combination of observations from three subsets: 279 Type Ia supernovae from Pan-STARRS ($0.03 < z < 0.68$), samples from SDSS, SNLS, and various low- z samples from HST. This forms one of the largest combined set of Type Ia supernovae, totaling 1048 Type Ia supernovae with redshift intervals ranging from 0.01 to 2.26. The luminosity distance (d_L) calculated to this sample is obtained by considering the SHOES (Supernovae and H0 for the Equation of State) calibration, where the Hubble Constant, $H_0 = 73 \pm 1$ km/s/Mpc [70]. To obtain the luminosity distance for each galaxy cluster, we employ the Gaussian process methodology to determine the central value along with its associated variance. The results for the gaussian process regression for d_L are shown in Fig.(2). In the following sections we present the main content of the 2HDM to be addressed in this work, and translate the above analysis to constrain the μ variation with redshift so as to exemplify how our approach is able to put bounds on Particle Physics models.

IV. THE TWO HIGGS DOUBLET MODEL

The 2HDM [36, 37] consists of introducing an additional scalar to the SM spectrum, transforming as a doublet under the weak isospin group and carrying hypercharge $Y = +1$. As usual, we choose the vev of both doublets to be along the direction of weak isospin $T^3 = -1/2$, the electrically neutral field components, so that expansion around the minimum energy configuration $\langle \Phi_i \rangle_0$ reads,

$$\Phi_i = \begin{pmatrix} \phi_i^+ \\ \phi_i^0 \end{pmatrix} = \begin{pmatrix} \phi_i^+ \\ \frac{1}{\sqrt{2}}(v_i + \rho_i + i\eta_i) \end{pmatrix}, \quad \langle \Phi_i \rangle_0 = \begin{pmatrix} 0 \\ v_i/\sqrt{2} \end{pmatrix}, \quad i = 1, 2. \quad (8)$$

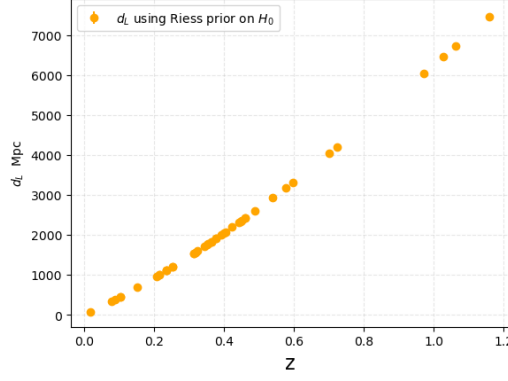


FIG. 2: Luminosity distances for the 44 galaxy clusters obtained through gaussian process regression using the value for the Hubble constant, H_0 , as given by Ref. [70].

In order to obtain a simplified scalar potential, we introduce a discrete symmetry for the scalar doublets (which will be justified later), $Z_2 : \Phi_1 \rightarrow -\Phi_1, \Phi_2 \rightarrow \Phi_2$. Then, allowing only a bilinear, $\Phi_1^\dagger \Phi_2 + \text{h.c.}$ term, which softly breaks the Z_2 symmetry so as to avoid the domain wall problem [71], the most general renormalizable, gauge, Lorentz and CP invariant scalar potential is written as,

$$\begin{aligned}
 V(\Phi_1, \Phi_2) = & m_1^2 \Phi_1^\dagger \Phi_1 + m_2^2 \Phi_2^\dagger \Phi_2 - m_{12}^2 (\Phi_1^\dagger \Phi_2 + \Phi_2^\dagger \Phi_1) + \frac{\lambda_1}{2} (\Phi_1^\dagger \Phi_1)^2 + \frac{\lambda_2}{2} (\Phi_2^\dagger \Phi_2)^2 \\
 & + \lambda_3 (\Phi_1^\dagger \Phi_1) (\Phi_2^\dagger \Phi_2) + \lambda_4 (\Phi_1^\dagger \Phi_2) (\Phi_2^\dagger \Phi_1) + \frac{\lambda_5}{2} \left[(\Phi_1^\dagger \Phi_2)^2 + (\Phi_2^\dagger \Phi_1)^2 \right]. \quad (9)
 \end{aligned}$$

After the electroweak spontaneous symmetry breaking (SSB), the bilinear terms in the scalar potential in Eq. (9) must be diagonalized, yielding the scalar mass spectrum of the model. From the original eight scalars, three are absorbed by the massive gauge bosons, W^\pm and Z^0 , while the five remaining get mixed to provide the mass eigenstates. The physical basis (mass basis) is achieved through the following rotations [72],

$$\begin{pmatrix} h \\ H \end{pmatrix} = R(\alpha) \begin{pmatrix} \rho_1 \\ \rho_2 \end{pmatrix}, \quad \begin{pmatrix} G \\ A \end{pmatrix} = R(\beta) \begin{pmatrix} \eta_1 \\ \eta_2 \end{pmatrix}, \quad \begin{pmatrix} G^\pm \\ H^\pm \end{pmatrix} = R(\beta) \begin{pmatrix} \phi_1^\pm \\ \phi_2^\pm \end{pmatrix}. \quad (10)$$

Where, each of the rotation matrices, $R(\theta)$, with $\theta = \alpha, \beta$ can be written as,

$$R(\theta) \equiv \begin{pmatrix} \cos \theta & \sin \theta \\ -\sin \theta & \cos \theta \end{pmatrix}, \quad (11)$$

with

$$\tan(2\alpha) \equiv \frac{-2m_{12}^2 v_1 v_2 + 2\lambda_{345} v_1^2 v_2^2}{m_{12}^2 (v_2^2 - v_1^2) + \lambda_1 v_1^3 v_2 - \lambda_2 v_1 v_2^3}; \quad \tan \beta \equiv \frac{v_2}{v_1}, \quad (12)$$

where we have defined $\lambda_{345} \equiv \lambda_3 + \lambda_4 + \lambda_5$.

The scalar's mass spectrum then becomes:

$$m_h^2 = \frac{1}{2} (\Delta_\rho - \delta_\rho); \quad m_H^2 = \frac{1}{2} (\Delta_\rho + \delta_\rho); \quad m_A^2 = \left[\frac{m_{12}^2}{v_1 v_2} - \lambda_5 \right] (v_1^2 + v_2^2); \quad (13)$$

$$m_{H^\pm}^2 = \left[\frac{m_{12}^2}{v_1 v_2} - \frac{1}{2} (\lambda_4 + \lambda_5) \right] (v_1^2 + v_2^2), \quad (14)$$

where we have defined,

$$\Delta_\rho = \frac{m_{12}^2 (v_1^2 + v_2^2)}{v_1 v_2} + \lambda_1 v_1^2 + \lambda_2 v_2^2 \quad \text{and} \quad \delta_\rho = \left[\left(\frac{m_{12}^2 (v_1^2 - v_2^2)}{v_1 v_2} - \lambda_1 v_1^2 + \lambda_2 v_2^2 \right)^2 + 4(m_{12}^2 - \lambda_{345} v_1 v_2)^2 \right]^{\frac{1}{2}}.$$

In the above description, the three Goldstone bosons are denoted by, G and G^\pm , which constitute the longitudinal polarization of the massive gauge bosons, whose masses are the same as in the SM, with the same vev but now written as, $v \equiv \sqrt{v_1^2 + v_2^2} = 246$ GeV. The remaining scalar fields, h and H , are electrically neutral CP even, with $m_H > m_h$, while A is a pseudoscalar (CP odd), which together with the two charged scalars, H^\pm , are the physical scalars in the spectrum of the theory. For our purposes, the relevant interactions for future computations come from the Yukawa Lagrangian, responsible for fermion mass generation,

$$-\mathcal{L}_{\text{yukawa}}^{\text{2HDM}} = y_{ij}^{1e}(\bar{L}^i\Phi_1)e_R^j + y_{ij}^{1d}(\bar{Q}^i\Phi_1)d_R^j + y_{ij}^{1u}(\bar{Q}^i\tilde{\Phi}_1)u_R^j + y_{ij}^{2e}(\bar{L}^i\Phi_2)e_R^j + y_{ij}^{2d}(\bar{Q}^i\Phi_2)d_R^j + y_{ij}^{2u}(\bar{Q}^i\tilde{\Phi}_2)u_R^j + \text{h.c.}, \quad (15)$$

therefore,

$$M_{ij}^f = \frac{v_1}{\sqrt{2}}y_{ij}^{1f} + \frac{v_2}{\sqrt{2}}y_{ij}^{2f}, \quad (16)$$

where, L^i and Q^i represent the usual SM left-handed lepton and quark doublets, respectively, while e_R , u_R and d_R , their corresponding singlet right-handed partners. y_{ij} denotes the matrix elements of dimensionless Yukawa couplings and M refers to the fermionic mass matrix (not necessarily diagonal). Each term is summed over the family indices i and j and we defined, $\tilde{\Phi}_i \equiv i\sigma_2\Phi_i^*$.

Observe that, differently from the SM, here we have two unrelated sources of contributions to fermion mass terms, one from the matrix v_1y^{1f} and another from v_2y^{2f} . The bold implication is that there is no change of basis that diagonalizes both terms simultaneously, leading to Flavor Changing Neutral Currents (FCNC) in the fermion-scalar couplings. The fact that such interactions are experimentally unobserved, calls for some arrangement to strongly suppress them. This can be achieved if we demand that each fermion mass matrix come from only one of the scalar doublets, so that diagonalizing all fermion mass matrices, M^f , implies the automatic diagonalization of $y^{1,2}$ (with the corresponding change from fermion interaction eigenstates to mass eigenstates) and, consequently, the disappearance of FCNC. This mechanism is known as Natural Flavor Conservation (NFC) [73, 74]. The easiest way to implement that is through the introduction of an extra symmetry, under which the scalar doublets transform differently, so that each fermion (also transforming under this symmetry) can couple to only one of the doublets. Our choice for that is a discrete Z_2 symmetry such that, $\Phi_1 \rightarrow -\Phi_1$, $\Phi_2 \rightarrow \Phi_2$. This is the reason we omitted odd terms in either of the scalar doublets in the scalar potential, Eq. (9), except for the soft Z_2 breaking term as we mentioned before.

The convention is to take all the fermion doublets, as well as singlet up-type quarks (u_R), to transform trivially, so that the up-type quarks always couple to Φ_2 and we are left to decide which of the scalar doublets couples to the singlet down-type fermions (right-handed down-type quarks d_R and charged leptons e_R). In the scenario we choose to work here, called **lepton-specific** 2HDM (or LS2HDM for short), d_R is assigned positive parity under Z_2 (so that both, d_R and u_R couple to Φ_2 , only) and e_R is assigned negative parity (couples to Φ_1 , only). We can then rewrite the Yukawa Lagrangian, Eq. (15), in the mass basis for both, scalars and fermions [72],

$$\begin{aligned} -\mathcal{L}_{\text{yukawa}}^{\text{LS2HDM}} &= \sum_{f=u,d,e} m_f \bar{f}f + \sum_{f=u,d,e} \frac{m_f}{v} (\xi_h^f \bar{f}f h + \xi_H^f \bar{f}f H - i\xi_A^f \bar{f}\gamma_5 f A) \\ &- \left[\frac{\sqrt{2}}{v} \bar{u} V_{ud} (m_u \xi_A^u P_L + m_d \xi_A^d P_R) d H^+ + \frac{\sqrt{2} m_e \xi_A^e}{v} \bar{\nu}_L e_R H^+ + \text{h.c.} \right], \end{aligned} \quad (17)$$

with,

$$\xi_h^u = \xi_h^d = s_\alpha/s_\beta, \quad \xi_h^e = c_\alpha/c_\beta, \quad \xi_H^u = \xi_H^d = c_\alpha/s_\beta, \quad \xi_H^e = -s_\alpha/c_\beta, \quad \xi_A^u = -\xi_A^d = (t_\beta)^{-1}, \quad \xi_A^e = t_\beta,$$

where we defined $c_\theta \equiv \cos\theta$, $s_\theta \equiv \sin\theta$ and $t_\theta \equiv \tan\theta$ for shorthand notation, the sum is over all up-type and down-type fermions (leptons and quarks) and the coefficient V_{ud} denotes the appropriate element of the CKM matrix. There is a linear combination of the neutral scalars that corresponds to the SM Higgs boson [72],

$$H^{\text{SM}} \sim h \cos(\beta - \alpha) + H \sin(\beta - \alpha) \quad (18)$$

which allows us to choose between h and H to represent the observed Higgs boson, H^{SM} , with mass around 125 GeV, and consistent with SM predictions for its interactions with fermions, implying a constraint on the mixing angles α and β . Here we make the choice of h , the lighter scalar, to be the observed Higgs boson, so that $\alpha = \beta$, from now on. We are now, prepared to obtain a constraint on this model from the bounds on μ varying with the redshift as inferred from the gas mass fraction in galaxy clusters, as we present next.

V. ANALYSIS AND RESULTS

Now we are going to obtain bounds on the variation of the electron to proton mass ratio by comparing the observed gas mass fraction within galaxy clusters to the theoretical gas mass fraction which is predicted by cosmological models as explained earlier in Sec. II. From the 44 data-points we inferred a variation of μ ($\Delta\mu$), such as,

$$\Delta\mu = 1.77 \times 10^{-2} \pm 9.8 \times 10^{-2}. \quad (19)$$

Although the constraints are not as restrictive as those obtained through quasar absorption spectra, the measurements are in agreement within 1σ confidence level. It is worth noting that the physics involved here is completely different. The techniques used to measure $\mu(z)$ in quasar spectroscopy rely on the hyperfine transition of molecules such as H_2 , FeII , and SiII [75, 76], with this transition being proportional to the ratio $\frac{\alpha_{EM}^2 g_p}{\mu}$ and the effective radius of the nucleus. In this scenario, the ratio between the mass of the electron and the mass of the proton is not directly measured; rather, it is the ratio between the mass of the electron and the effective mass of the nucleus [12]. A measurement using the Eq. (4) obtained through X-ray emission from ICM plasma, which consists predominantly of hydrogen ions, is a more direct measurement.

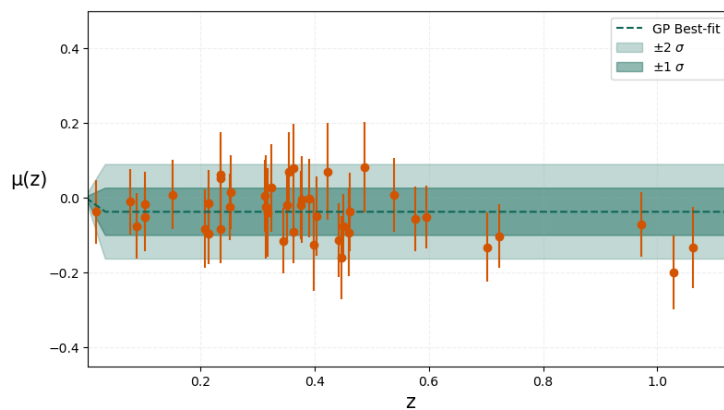


FIG. 3: Reconstruction of $\mu(z)$ via gaussian processes regression for the GMF data using Riess' prior for luminosity distance. Best fit curve and 1 and 2 σ interval of confidence.

Gaussian Processes (GPs) offer a method for reconstructing a function from observational data without assuming a specific parametrization. The GP reconstruction process involves selecting a prior mean function and a covariance function that quantifies the correlation between the values of the dependent variable in the reconstruction, which are characterized by a set of hyperparameters such as the signal variance σ and the characteristic length scale l . Unlike regular parameters, hyperparameters do not dictate the shape of a function, rather, they characterize typical variations in the reconstructed function. l roughly represents the scale over which significant changes occur in the function values across z , while σ indicates the typical magnitude of these alterations [77]. While more complex covariance functions may involve additional hyperparameters, in this work we used a covariance function that solely incorporate σ and l . To reconstruct $\mu(z)$, we choose zero as the prior mean function to avoid biased results and also require that $\mu(z)$ matches the laboratory value (at redshift 0), we show the plot of our reconstruction in Fig. (3) along with a Gaussian kernel serving as the covariance function, as follows,

$$k(z, z') = \sigma^2 \exp\left(-\frac{(z - z')^2}{2l^2}\right). \quad (20)$$

To perform the GP we used the algorithm scikit-learn [78]. Finally, we defined a likelihood function that compares the values of $\mu(z)$ obtained through GPR with the experimentally measured value μ_0 ,

$$L(y_e, v_2, \cot\beta(z)) = \prod_{i=1}^n \frac{1}{\sqrt{2\pi\sigma_i^2}} \exp\left(-\frac{(\mu_{\text{GPR}}(z_i) - \mu_0(z_i))^2}{2\sigma_i^2}\right). \quad (21)$$

We then chose an initial distribution for the electron Yukawa coupling, y_e , the vev of Φ_1 , v_1 , and the ratio of vevs in the 2HDM, $\tan\beta(z)$, and then implemented a MCMC. Using the diagonalized Yukawa coupling for electrons in

the LS2HDM, obtained from Eqs. (15,16), and assuming that any variation in μ with z arises from $v_1(z)$, that is, the proton mass remains constant, we obtain,

$$\mu(z) = \frac{y_e v_2}{\sqrt{2} m_p (\Lambda_{\text{QCD}})} \cot \beta(z). \quad (22)$$

This expression, evaluated at $z = 0$, provides constraints for the Yukawa coupling of the electron, y_e , for the $\cot \beta_0$, and the vev, v_2 . The samples generated provide us with the best estimates for the parameters as given in Fig. (4), along with the conditional 2D regions for the confidence intervals. The results for the constrained parameters are summarized in Table I.

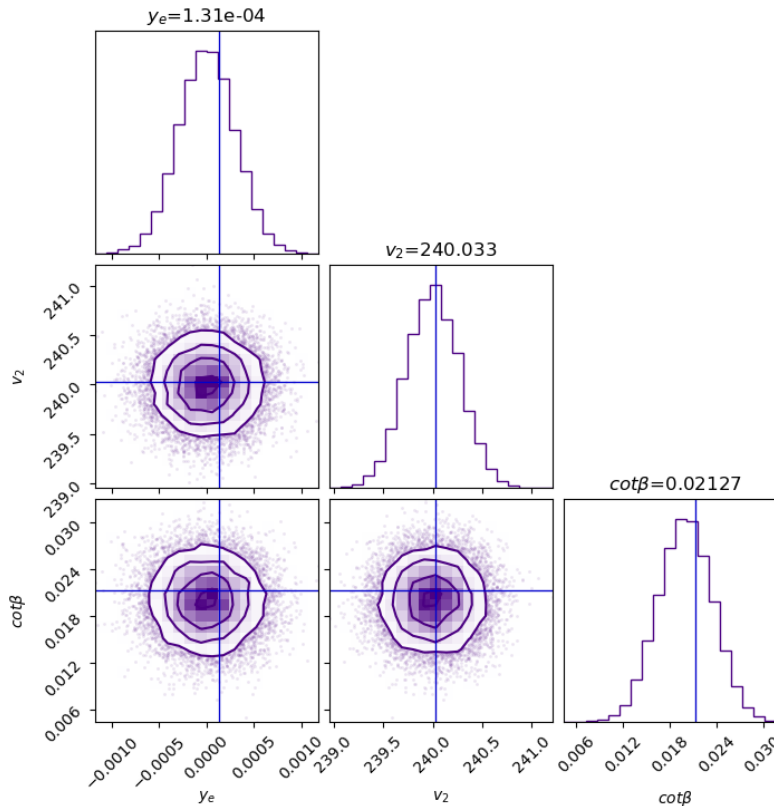


FIG. 4: Constraints on y_e , v_2 , and $\cot \beta$ from $\mu(z)$ obtained using Riess' prior. The diagonal plots represent 1-D marginalized likelihood distributions of each parameter present and off-diagonal contours are 68%, 95%, and 99% 2-D marginalized confidence regions.

Parameter	Value
$y_e (10^{-4})$	$1.31 \cdot 10^{-4} \pm 0.00095$
$v_2 (\text{GeV})$	240.033 ± 0.21
$\cot \beta$	0.02127 ± 0.0029

TABLE I: Summary of the best values for the model's parameters obtained from our MCMC sampling.

This constitutes the main result of our work. Next we compute the contribution of LS2HDM to the muon anomalous magnetic moment and gather additional constraints to the model so as to find the favorable parameter space that is constrained by $\mu(z)$.

VI. LS2HDM AND THE MUON ANOMALOUS MAGNETIC MOMENT

There is, currently, a discrepancy between the muon anomalous magnetic moment, $a_\mu \equiv (g-2)_\mu$, predicted by the SM and its experimental value, $\Delta a_\mu^{obs} \equiv a_\mu^{EXP} - a_\mu^{SM} = (25.1 \pm 5.9) \cdot 10^{-10}$ [34, 35]. We show here that our model is capable of accounting for that difference at 2σ .

The most important contributions to $(g-2)_\mu$ from the LS2HDM are given by the diagrams in figure 5, with ϕ representing the neutral scalars h, H, A . Here, h is chosen to be the SM Higgs, with mass, $m_h = 125$ GeV, whose contribution is already considered in the theoretical prediction so it does not enter in the computation of the deviation. Furthermore, the charged scalar contribution is insignificant, so it will not be considered here, meaning that we only take H and A into account. The first one loop diagram in Fig (5) results in [79],

$$\Delta a_\mu^{1\text{ loop}} = \frac{1}{8\pi^2} \left(\frac{m_\mu}{v}\right)^2 \left\{ (\xi_H^\mu)^2 \left[2I_1 \left(\frac{m_\mu^2}{m_H^2}\right) - I_2 \left(\frac{m_\mu^2}{m_H^2}\right) \right] - (\xi_A^\mu)^2 I_2 \left(\frac{m_\mu^2}{m_A^2}\right) \right\}, \quad (23)$$

with,

$$I_1(x) = 1 + \frac{1-2x}{2x\sqrt{1-4x}} \ln \left(\frac{1+\sqrt{1-4x}}{1-\sqrt{1-4x}} \right) + \frac{1}{2x} \ln x \approx x \left(-\frac{3}{2} - \ln x \right) + x^2 \left(-\frac{16}{3} - 4 \ln x \right) + \mathcal{O}(x^3), \quad (24)$$

$$I_2(x) = \frac{1}{2} + \frac{1}{x} + \frac{1-3x}{2x^2\sqrt{1-4x}} \ln \left(\frac{1+\sqrt{1-4x}}{1-\sqrt{1-4x}} \right) + \frac{1-2x}{2x^2} \ln x \approx x \left(-\frac{11}{6} - \ln x \right) + x^2 \left(-\frac{89}{12} - 5 \ln x \right) + \mathcal{O}(x^3). \quad (25)$$

At one loop, H contributes positively and A , negatively [80], so that the overall contribution is not enough to explain the anomaly. For this reason we include the second diagram in Fig. (5), a special type of two loop contribution called Barr-Zee diagram, which yields [79],

$$\Delta a_\mu^{\text{Barr-Zee}} = -\frac{2\alpha}{\pi} \frac{1}{8\pi^2} \left(\frac{m_\mu}{v}\right)^2 \sum_f N_c^f Q_f^2 \left\{ \xi_H^\mu \xi_H^f f \left(\frac{m_f^2}{m_H^2}\right) - \xi_A^\mu \xi_A^f g \left(\frac{m_f^2}{m_A^2}\right) \right\} \quad (26)$$

$$f(z) = \frac{z}{2} \int_0^1 dx \frac{1-2x(1-x)}{x(1-x)-z} \ln \left(\frac{x(1-x)}{z} \right) \quad (27)$$

$$g(z) = \frac{z}{2} \int_0^1 dx \frac{1}{x(1-x)-z} \ln \left(\frac{x(1-x)}{z} \right) \quad (28)$$

Here H contributes negatively and A , positively [80]. We sum over all the fermions, f , in the loop, each one characterized by its color number, N_c^f (which is equal to 3 for quarks and zero for leptons), and its electric charge (multiple of unit positron charge), Q_f .

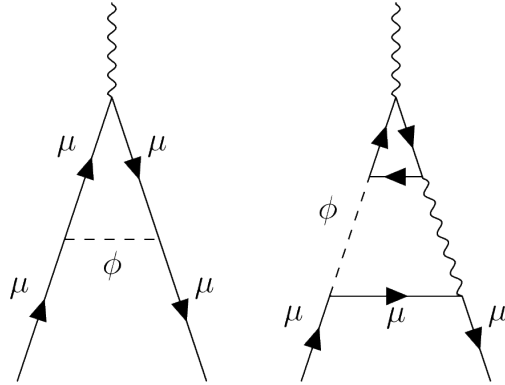


FIG. 5: Neutral scalar contributions to muon, $(g-2)_\mu$ (the wiggly lines are photon ones).

The above expressions depend on m_H , m_A and $\tan\beta$, which are in principle hard to constrain because (considering $\beta = \alpha$) the quark couplings from Eq. (17) are proportional to $\cot\beta \ll 1$. This means that hadronic cross sections are attenuated and thus incapable of providing bounds for the 2HDM masses. So it becomes necessary to establish model-dependent bounds on these parameters. We follow here the model suggested by Ref. [80], which uses lepton universality constraints, the CDF W boson mass results and muonic $g-2$ measurements to probe the allowed parameter space (as well as the requirement of vacuum stability, perturbativity and unitarity in the wrong sign scenario). The $h \rightarrow AA$ decay channel is considered, adding the constraint $m_h \geq 2m_A$.

The regions in parameter space that meet these requirements and keep $\Delta a_\mu^{2\text{HDM}}(m_H, m_A, t_\beta) = \Delta a_\mu^{1\text{ loop}} + \Delta a_\mu^{\text{Barr-Zee}}$ inside 1σ , 2σ or 3σ deviation from $\Delta a_\mu^{\text{obs}} = (25.1 \pm 5.9) \cdot 10^{-10}$ are shown in Figs. (6) and (7), displayed as green bands. In Fig. (6), we present the predictions of $\tan\beta$ against the pseudoscalar mass, m_A , keeping the mass of the heavier scalar, m_H , fixed at $m_H = 300$ GeV. We take into account the bounds stemming from our astrophysical analysis of $\mu(z)$ in Table I, representing $\cot\beta = 0.0213 \pm 0.0029$ (light gray band). We see that a light pseudoscalar is favored, with m_A ranging from around 10 to 50 GeV. As for the Fig. (7), our prediction for $\Delta a_\mu^{2\text{HDM}}$ is plotted as a function of m_A with $m_H = 300$ GeV. We kept $\tan\beta$ fixed with central value $\tan\beta = 47$ (solid purple curve) and the limiting values at $\pm 1\sigma_{\tan\beta} = \pm 6.4$ (dashed purple curves). The green bands are the observed $(g-2)_\mu$ discrepancy at 1σ , 2σ and 3σ . From this figure we conclude that the neutral scalar contributions can solve the muon anomaly at 1σ when $m_A \gtrsim 10$ GeV. The critical point at $m_A \approx 10.6$ GeV is due to the competition between the one loop (negative) and Barr-Zee (positive) contributions.

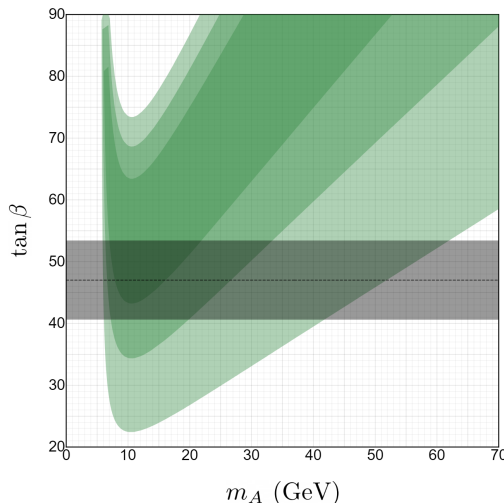


FIG. 6: Constraints on 2HDM parameters m_A and $\tan\beta$ using the $(g-2)_\mu$ prediction of LS2HDM (m_H is fixed at 300 GeV). The green regions represent, from darker to lighter, 1σ , 2σ and 3σ , where a χ^2 distribution is adopted. The region in light gray represents $\cot\beta = 0.0213 \pm 0.0029$ from Table I.

Just for completeness, we use some additional constraints from Ref. [80] that give $m_{H^\pm} \gtrsim m_H$, besides solving the $(g-2)_\mu$ discrepancy and the W mass anomaly simultaneously. For that, we superpose our results from the $\mu(z)$ bounds on $\tan\beta$ in the LS2HDM (table I) to their results on $(g-2)_\mu$, universality tests through τ -decay and $Z \rightarrow \bar{l}l$ (Z decay into a pair of leptons), as well as the scalar mass difference, $\Delta \equiv m_{H^\pm} - m_H$, constrained by the requirement that it solves the W mass anomaly [81]. We see from Fig. (8) that these extra bounds are compatible with our constraints on $\tan\beta$ in the 1σ range $40.6 \leq \tan\beta \leq 53.4$, covering the central value obtained before with a small variation depending on the heavier neutral scalar mass. The first panel in that figure is for a heavier Higgs, $m_H = 300$ GeV, while the second one is for $m_H = 400$ GeV. The upper bounds on $\tan\beta$ from τ -decay and $Z \rightarrow \bar{l}l$ are shown as full and dashed lines for different choices of the scalar mass difference, Δ . Observe that their results for the $(g-2)_\mu$, sketched in brown, is a little bit different from ours because they use only the lepton τ in the Barr-Zee loop, while we summed over all the SM fermions.

VII. CONCLUSIONS

In this work, we analyze the expression for the gas mass fraction of a galaxy cluster and found that $f_{\text{gas}} \propto (1 + \mu)^2$. Thus, by combining type Ia Supernovae observations with gas mass fraction measurement data from 44 galaxy clusters,

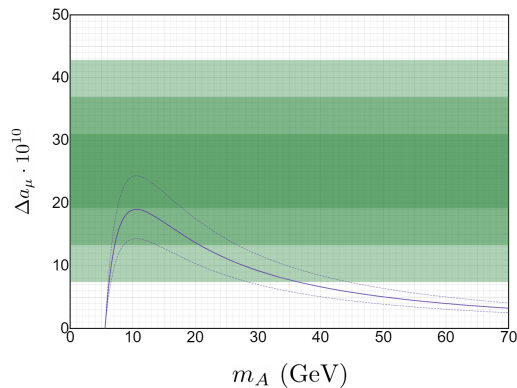


FIG. 7: $\Delta a_\mu^{2\text{HDM}}$ as a function of m_A with $m_H = 300$ GeV. We took the central value $\tan \beta = 47$ (solid purple curve) and the limiting values at $1\sigma_{\tan \beta} = 6.4$ (dashed purple curves). The green bands are the observed $(g-2)_\mu$ discrepancy at 1σ , 2σ and 3σ .

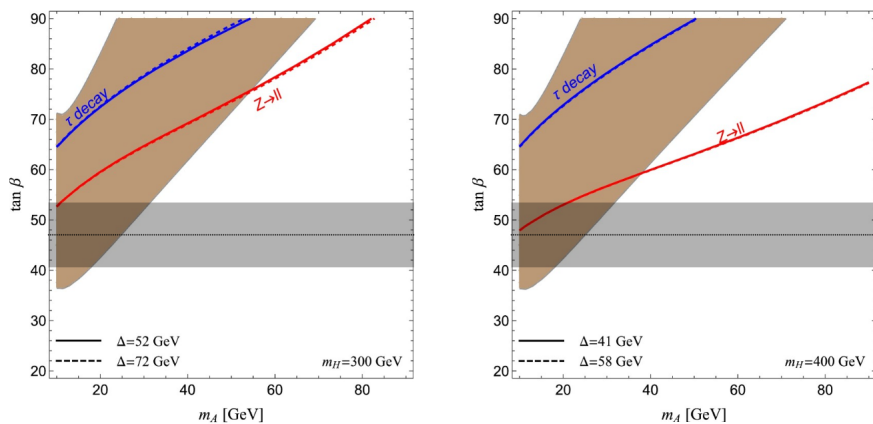


FIG. 8: Constraints given by [80]. The 2σ region allowed by the muon $g-2$ is sketched in brown. The coloured lines give upper bounds on $\tan \beta$ from lepton universality tests, exploring both τ decay and Z decay in any pair of leptons. The full and dashed lines are associated with the lower and upper bounds on $\Delta \equiv m_{H^\pm} - m_H$, respectively, and we superimposed the region in light gray to represent our astrophysical results.

we put constraints on a possible variation of the electron-to-proton mass ratio, $\Delta\mu$ given in Eq. (19). Additionally, using a Gaussian regression process, we reconstructed a $\mu(z)$ curve, given in Eq. (22), which allows us to impose limits on models beyond the electroweak SM of particle physics. In order to expose our approach, we employed a particular extension of the scalar sector of the SM by an extra Higgs doublet and an additional discrete Z_2 symmetry, resulting in the two-Higgs doublet model in the scenario of lepton-specific coupling, which we called LS2HDM, presented in Sec. IV. This choice is made not only for simplicity but to attach some useful meaning to a class of well studied models in literature. We were able to translate the results on $\mu(z)$ into constraints on the parameters of the model, namely the $\cot \beta$ (reverted to $\tan \beta$), v_2 and y_e (see table I, finding their optimal values from a MCMC sampling).

These constraints, when further contrasted with the possibility of the model to account for the discrepancy between experimental and SM theoretical values of the anomalous muon magnetic moment, $(g-2)_\mu$, resulted in a robust set of bounds on the parameters, favoring a rather light pseudoscalar, with $m_A \gtrsim 10$ GeV and the heavier scalar with mass around $300 \leq m_H \leq 400$ GeV. This last conclusions we obtained by gathering existing bounds [80] on the model when τ -decay and $Z \rightarrow \bar{l}l$ are considered together with the accommodation of the W-mass anomaly as seen by CDF-collaboration [81].

Finally, we stress that the main point of this work was to probe a complimentary approach to Particle Physics models from an interface with Astrophysics and Cosmology, which, in our case, derived from the gas properties in galactic clusters. Our conclusions add to unveil the importance of seeking new constraints for non-standard physics in places beyond Particle Physics accelerators only, and confirm that the large-scale structures of the universe might contain more information than we have previously thought. In the years ahead, there will be a substantial rise in both

the quantity and quality of observations made possible by instruments like the eROSITA telescope, a Russian-German collaboration. This progress will enable more comprehensive statistical analyses. Consequently, it will be feasible to achieve more restrictive limits by using the methodology outlined in this article.

ACKNOWLEDGEMENT

PSRS would like to thank the financial support from Conselho Nacional de Desenvolvimento Científico e Tecnológico (CNPq) under the project No. 309650/2019-4 and the support of UFPB through an internal project PIA16656-2023; RFLH thanks the financial support from the Conselho Nacional de Desenvolvimento Científico e Tecnológico (CNPq) under the project No. 308550/2023-47; RGA thanks the financial support from UFPB through PIBIC-CNPq under the project No. PIA16656-2023.

-
- [1] P. A. M. DIRAC, *Nature* volume **139**, 323 (1937).
 - [2] V. A. Dzuba, V. V. Flambaum, and J. K. Webb, *Phys. Rev. A* **59**, 230 (1999), URL <https://link.aps.org/doi/10.1103/PhysRevA.59.230>.
 - [3] Y. Fujii, A. Iwamoto, T. Fukahori, T. Ohnuki, M. Nakagawa, H. Hidaka, Y. Oura, and P. Möller, *Nuclear Physics B* **573**, 377–401 (2000), ISSN 0550-3213, URL [http://dx.doi.org/10.1016/S0550-3213\(00\)00038-9](http://dx.doi.org/10.1016/S0550-3213(00)00038-9).
 - [4] V. V. Flambaum and A. F. Tedesco, *Phys. Rev. C* **73**, 055501 (2006), URL <https://link.aps.org/doi/10.1103/PhysRevC.73.055501>.
 - [5] K. A. Olive, M. Pospelov, Y.-Z. Qian, G. Manhès, E. Vangioni-Flam, A. Coc, and M. Cassé, *Phys. Rev. D* **69**, 027701 (2004), URL <https://link.aps.org/doi/10.1103/PhysRevD.69.027701>.
 - [6] A. F. M. Fiorenzano, G. Vladilo, and P. Bonifacio, *Search for alpha variation in wves spectra: Analysis of c iv and si iv doublets towards qso 1101-264* (2004), astro-ph/0312270.
 - [7] P. Tzanavaris, J. K. Webb, M. T. Murphy, V. V. Flambaum, and S. J. Curran, *Physical Review Letters* **95** (2005), ISSN 1079-7114, URL <http://dx.doi.org/10.1103/PhysRevLett.95.041301>.
 - [8] P. Molaro, M. Centurión, J. B. Whitmore, T. M. Evans, M. T. Murphy, I. I. Agafonova, P. Bonifacio, S. D’Odorico, S. A. Levshakov, S. Lopez, et al., *Astronomy & Astrophysics* **555**, A68 (2013), ISSN 1432-0746, URL <http://dx.doi.org/10.1051/0004-6361/201321351>.
 - [9] M. T. Murphy, A. L. Malec, and J. X. Prochaska, *Monthly Notices of the Royal Astronomical Society* **461**, 2461–2479 (2016), ISSN 1365-2966, URL <http://dx.doi.org/10.1093/mnras/stw1482>.
 - [10] J.-P. Uzan, *Rev. Mod. Phys.* **75**, 403 (2003), URL <https://link.aps.org/doi/10.1103/RevModPhys.75.403>.
 - [11] J. D. Barrow, *Physical Review D* **71** (2005), ISSN 1550-2368, URL <http://dx.doi.org/10.1103/PhysRevD.71.083520>.
 - [12] C. J. A. P. Martins, *Reports on Progress in Physics* **80**, 126902 (2017), ISSN 1361-6633, URL <http://dx.doi.org/10.1088/1361-6633/aa860e>.
 - [13] C. Bambi, *Search for variations of fundamental constants* (2022), 2210.11959.
 - [14] H. Wei, X.-P. Ma, and H.-Y. Qi, *Physics Letters B* **703**, 74 (2011), ISSN 0370-2693, URL <https://www.sciencedirect.com/science/article/pii/S037026931100846X>.
 - [15] T. Harko, F. S. N. Lobo, and O. Minazzoli, *Phys. Rev. D* **87**, 047501 (2013), URL <https://link.aps.org/doi/10.1103/PhysRevD.87.047501>.
 - [16] A. Hees, O. Minazzoli, and J. Larena, *Phys. Rev. D* **90**, 124064 (2014), URL <https://link.aps.org/doi/10.1103/PhysRevD.90.124064>.
 - [17] T. Damour and A. Polyakov, *Nuclear Physics B* **423**, 532–558 (1994), ISSN 0550-3213, URL [http://dx.doi.org/10.1016/0550-3213\(94\)90143-0](http://dx.doi.org/10.1016/0550-3213(94)90143-0).
 - [18] C. Martins, P. Vielzeuf, M. Martinelli, E. Calabrese, and S. Pandolfi, *Physics Letters B* **743**, 377–382 (2015), ISSN 0370-2693, URL <http://dx.doi.org/10.1016/j.physletb.2015.03.002>.
 - [19] H. Davoudiasl and P. P. Giardino, *Physics Letters B* **788**, 270–273 (2019), ISSN 0370-2693, URL <http://dx.doi.org/10.1016/j.physletb.2018.11.041>.
 - [20] D. Brzemiński, Z. Chacko, A. Dev, and A. Hook, *Phys. Rev. D* **104**, 075019 (2021), URL <https://link.aps.org/doi/10.1103/PhysRevD.104.075019>.
 - [21] S. Galli, *Physical Review D* **87** (2013), ISSN 1550-2368, URL <http://dx.doi.org/10.1103/PhysRevD.87.123516>.
 - [22] I. de Martino, C. J. A. P. Martins, H. Ebeling, and D. Kocevski, *Phys. Rev. D* **94**, 083008 (2016), URL <https://link.aps.org/doi/10.1103/PhysRevD.94.083008>.
 - [23] I. De Martino, C. J. A. P. Martins, H. Ebeling, and D. Kocevski, *Universe* **2** (2016), ISSN 2218-1997, URL <https://www.mdpi.com/2218-1997/2/4/34>.
 - [24] L. Colaço, R. Holanda, R. Silva, and J. Alcaniz, *Journal of Cosmology and Astroparticle Physics* **2019**, 014–014 (2019), ISSN 1475-7516, URL <http://dx.doi.org/10.1088/1475-7516/2019/03/014>.
 - [25] R. F. L. Holanda, V. C. Busti, L. R. Colaço, J. S. Alcaniz, and S. J. Landau, *JCAP* **2016**, 055 (2016), 1605.02578.
 - [26] L. R. Colaço, R. F. L. Holanda, R. Silva, and J. S. Alcaniz, *JCAP* **2019**, 014 (2019), 1901.10947.

- [27] Z.-E. Liu, W.-F. Liu, T.-J. Zhang, Z.-X. Zhai, and K. Bora, *The Astrophysical Journal* **922**, 19 (2021), ISSN 1538-4357, URL <http://dx.doi.org/10.3847/1538-4357/ac2150>.
- [28] G. Aad et al. (ATLAS), *Phys. Lett. B* **716**, 1 (2012), 1207.7214.
- [29] S. Chatrchyan et al. (CMS), *Phys. Lett. B* **716**, 30 (2012), 1207.7235.
- [30] G. Aad et al. (ATLAS), *Nature* **607**, 52 (2022), [Erratum: *Nature* 612, E24 (2022)], 2207.00092.
- [31] G. Bertone and D. Hooper, *Rev. Mod. Phys.* **90**, 045002 (2018), 1605.04909.
- [32] P. F. de Salas, D. V. Forero, S. Gariazzo, P. Martínez-Miravé, O. Mena, C. A. Ternes, M. Tórtola, and J. W. F. Valle, *JHEP* **02**, 071 (2021), 2006.11237.
- [33] F. Capozzi, E. Di Valentino, E. Lisi, A. Marrone, A. Melchiorri, and A. Palazzo, *Phys. Rev. D* **95**, 096014 (2017), [Addendum: *Phys.Rev.D* 101, 116013 (2020)], 2003.08511.
- [34] L. Cotrozzi and M. Sorbara, in *Proceedings of 41st International Conference on High Energy physics — PoS(ICHEP2022)* (2022), vol. 414, p. 749.
- [35] A. Keshavarzi, K. S. Khaw, and T. Yoshioka, *Nuclear Physics B* **975**, 115675 (2022), ISSN 0550-3213, URL <http://dx.doi.org/10.1016/j.nuclphysb.2022.115675>.
- [36] G. Branco, P. Ferreira, L. Lavoura, M. Rebelo, M. Sher, and J. P. Silva, *Physics Reports* **516**, 1 (2012), ISSN 0370-1573, theory and phenomenology of two-Higgs-doublet models, URL <https://www.sciencedirect.com/science/article/pii/S0370157312000695>.
- [37] L. Wang, J. M. Yang, and Y. Zhang, *Commun. Theor. Phys.* **74**, 097202 (2022), 2203.07244.
- [38] S. P. Martin, *Adv. Ser. Direct. High Energy Phys.* **18**, 1 (1998), hep-ph/9709356.
- [39] M. A. Luty, in *Theoretical Advanced Study Institute in Elementary Particle Physics: Physics in $D \geq 4$* (2005), pp. 495–582, hep-th/0509029.
- [40] V. S. Mummidi, P. Lamba, and S. K. Vempati, *Indian J. Phys.* **97**, 3315 (2023), 2306.05797.
- [41] T. D. Lee, *Phys. Rev. D* **8**, 1226 (1973).
- [42] A. I. Bochkarev, S. V. Kuzmin, and M. E. Shaposhnikov, *Phys. Lett. B* **244**, 275 (1990).
- [43] N. Turok and J. Zadrozny, *Nucl. Phys. B* **358**, 471 (1991).
- [44] J. M. Cline and P.-A. Lemieux, *Phys. Rev. D* **55**, 3873 (1997), hep-ph/9609240.
- [45] L. Fromme, S. J. Huber, and M. Seniuch, *JHEP* **11**, 038 (2006), hep-ph/0605242.
- [46] J. M. Cline, K. Kainulainen, and M. Trott, *Journal of High Energy Physics* **2011** (2011), ISSN 1029-8479, URL [http://dx.doi.org/10.1007/JHEP11\(2011\)089](http://dx.doi.org/10.1007/JHEP11(2011)089).
- [47] G. C. Dorsch, S. J. Huber, and J. M. No, *JHEP* **10**, 029 (2013), 1305.6610.
- [48] B. Abi, T. Albahri, S. Al-Kilani, D. Allspach, L. Alonzi, A. Anastasi, A. Anisenkov, F. Azfar, K. Badgley, S. Baeßler, et al., *Physical Review Letters* **126** (2021), ISSN 1079-7114, URL <http://dx.doi.org/10.1103/PhysRevLett.126.141801>.
- [49] S. W. Allen, A. E. Evrard, and A. B. Mantz, *Ann. Rev. Astron. Astrophys.* **49**, 409 (2011), 1103.4829.
- [50] C. L. Sarazin, *X-ray emission from clusters of galaxies* (1988).
- [51] S. W. Allen, D. A. Rapetti, R. W. Schmidt, H. Ebeling, R. G. Morris, and A. C. Fabian, *Monthly Notices of the Royal Astronomical Society* **383**, 879 (2008), ISSN 0035-8711, <https://academic.oup.com/mnras/article-pdf/383/3/879/3466307/mnras0383-0879.pdf>, URL <https://doi.org/10.1111/j.1365-2966.2007.12610.x>.
- [52] Etori, S., Morandi, A., Tozzi, P., Balestra, I., Borgani, S., Rosati, P., Lovisari, L., and Terenziani, F., *A&A* **501**, 61 (2009), URL <https://doi.org/10.1051/0004-6361/200810878>.
- [53] A. B. Mantz, S. W. Allen, R. G. Morris, D. A. Rapetti, D. E. Applegate, P. L. Kelly, A. von der Linden, and R. W. Schmidt, *Monthly Notices of the Royal Astronomical Society* **440**, 2077 (2014), ISSN 0035-8711, <https://academic.oup.com/mnras/article-pdf/440/3/2077/23991383/stu368.pdf>, URL <https://doi.org/10.1093/mnras/stu368>.
- [54] I. Mendonça, K. Bora, R. Holanda, S. Desai, and S. Pereira, *Journal of Cosmology and Astroparticle Physics* **2021**, 034 (2021), ISSN 1475-7516, URL <http://dx.doi.org/10.1088/1475-7516/2021/11/034>.
- [55] I. Mendonça, K. Bora, R. Holanda, and S. Desai, *Journal of Cosmology and Astroparticle Physics* **2021**, 084 (2021), ISSN 1475-7516, URL <http://dx.doi.org/10.1088/1475-7516/2021/10/084>.
- [56] R. F. L. Holanda, S. H. Pereira, V. C. Busti, and C. H. G. Bessa, *Classical and Quantum Gravity* **34**, 195003 (2017), 1705.05439.
- [57] R. F. L. Holanda, S. H. Pereira, and S. Santos da Costa, *Phys. Rev. D* **95**, 084006 (2017), 1612.09365.
- [58] S. Sasaki, *Publications of the Astronomical Society of Japan* **48**, L119–L122 (1996), ISSN 2053-051X, URL <http://dx.doi.org/10.1093/pasj/48.6.L119>.
- [59] M. A. Dopita and R. S. Sutherland, *Astrophysics of the Diffuse Universe*, *Astronomy and Astrophysics Library* (Springer Berlin, Heidelberg, 2003).
- [60] P. J. E. Peebles, *Principles of Physical Cosmology* (1993).
- [61] F. M. White, *Fluid Mechanics* (McGraw-Hill, 2011), 7th ed.
- [62] N. Battaglia, J. R. Bond, C. Pfrommer, and J. L. Sievers, *Astrophys. J.* **777**, 123 (2013), 1209.4082.
- [63] S. Planelles, S. Borgani, K. Dolag, S. Etori, D. Fabjan, G. Murante, and L. Tornatore, *Mon. Not. R. Astron. Soc.* **431**, 1487 (2013), 1209.5058.
- [64] S. W. Allen, D. A. Rapetti, R. W. Schmidt, H. Ebeling, R. G. Morris, and A. C. Fabian, *Mon. Not. R. Astron. Soc.* **383**, 879 (2008), 0706.0033.
- [65] A. B. Mantz, R. G. Morris, S. W. Allen, R. E. A. Canning, L. Baumont, B. Benson, L. E. Bleem, S. R. Ehlert, B. Floyd, R. Herbonnet, et al., *Monthly Notices of the Royal Astronomical Society* **510**, 131–145 (2021), ISSN 1365-2966, URL <http://dx.doi.org/10.1093/mnras/stab3390>.

- [66] A. Krolewski and W. J. Percival, arXiv e-prints arXiv:2403.19236 (2024), 2403.19236.
- [67] X. Zheng, J.-Z. Qi, S. Cao, T. Liu, M. Biesiada, S. Miernik, and Z.-H. Zhu, *The European Physical Journal C* **79** (2019), ISSN 1434-6052, URL <http://dx.doi.org/10.1140/epjc/s10052-019-7143-3>.
- [68] D. E. Applegate, A. von der Linden, P. L. Kelly, M. T. Allen, S. W. Allen, P. R. Burchat, D. L. Burke, H. Ebeling, A. Mantz, and R. G. Morris, *Mon. Not. R. Astron. Soc.* **439**, 48 (2014), 1208.0605.
- [69] D. M. Scolnic, D. O. Jones, A. Rest, Y. C. Pan, R. Chornock, R. J. Foley, M. E. Huber, R. Kessler, G. Narayan, A. G. Riess, et al., *The Astrophysical Journal* **859**, 101 (2018), ISSN 1538-4357, URL <http://dx.doi.org/10.3847/1538-4357/aab9bb>.
- [70] A. G. Riess et al., *Astrophys. J. Lett.* **934**, L7 (2022), 2112.04510.
- [71] Y. B. Zeldovich, I. Y. Kobzarev, and L. B. Okun, *Zh. Eksp. Teor. Fiz.* **67**, 3 (1974).
- [72] T. Melo (2020), URL <https://repositorio.ufpb.br/jspui/handle/123456789/19693>.
- [73] E. A. Paschos, *Phys. Rev. D* **15**, 1966 (1977), URL <https://link.aps.org/doi/10.1103/PhysRevD.15.1966>.
- [74] S. L. Glashow and S. Weinberg, *Phys. Rev. D* **15**, 1958 (1977), URL <https://link.aps.org/doi/10.1103/PhysRevD.15.1958>.
- [75] W. Ubachs, J. Bagdonaite, E. J. Salumbides, M. T. Murphy, and L. Kaper, *Rev. Mod. Phys.* **88**, 021003 (2016), URL <https://link.aps.org/doi/10.1103/RevModPhys.88.021003>.
- [76] J. D. Barrow and J. a. Magueijo, *Phys. Rev. D* **72**, 043521 (2005), URL <https://link.aps.org/doi/10.1103/PhysRevD.72.043521>.
- [77] M. Seikel and C. Clarkson, arXiv preprint arXiv:1311.6678 (2013).
- [78] F. Pedregosa, G. Varoquaux, A. Gramfort, V. Michel, B. Thirion, O. Grisel, M. Blondel, P. Prettenhofer, R. Weiss, V. Dubourg, et al., *the Journal of machine Learning research* **12**, 2825 (2011).
- [79] F. J. Botella, F. Cornet-Gomez, C. Miró, and M. Nebot, *The European Physical Journal C* **82** (2022), ISSN 1434-6052, URL <http://dx.doi.org/10.1140/epjc/s10052-022-10893-x>.
- [80] J. Kim, *Physics Letters B* **832**, 137220 (2022), ISSN 0370-2693, URL <https://www.sciencedirect.com/science/article/pii/S0370269322003549>.
- [81] T. Aaltonen et al. (CDF), *Science* **376**, 170 (2022).